JOURNAL OF AGRICULTURAL AND FOOD CHEMISTRY

Article

pubs.acs.org/JAFC

Photo- and Thermodegradation of Anthocyanins from Grape and Purple Sweet Potato in Model Beverage Systems

Brian J. Song,[†] Teryn N. Sapper,[†] Claire E. Burtch,[†] Karen Brimmer,[§] Mark Goldschmidt,[§] and Mario G. Ferruzzi*,[†,‡]

[†]Department of Food Science, Purdue University, 745 Agriculture Mall Drive, West Lafayette, Indiana 47906, United States

[§]Sensient Colors Inc., 2515 North Jefferson, St. Louis, Missouri 63106, United States

[‡]Department of Nutrition Science, Purdue University, 700 West State Street, West Lafayette, Indiana 47907, United States

ABSTRACT: Recently, interest in the application of natural pigments to replace synthetic dyes in beverages has grown. The present study investigates the stability of anthocyanin-rich grape and purple sweet potato (PSP) extracts to photo- and thermostresses in ready-to-drink (RTD) beverage models including hot fill beverages with various concentrations of ascorbic acid, a preserved beverage, and a vitamin-enriched water beverage. Thermo- and photostresses were induced at 40, 60, and 80 °C and 250, 500, and 750 W/m^2, respectively. Qualitative and quantitative data on anthocyanin content were collected by pH differential assay and LC-MS. Increasing concentration of ascorbic acid caused more rapid degradation through thermostress, but had a protective effect through photostress. Additionally, PSP was significantly less stable than grape extract in the vitamin-enriched water model beverage through photostress. Furthermore, photostress caused the formation of monoacylated peonidins from diacylated peonidins.

KEYWORDS: *acylated anthocyanin, light, heat, kinetics, ascorbic acid*

INTRODUCTION

With increasing public awareness of the potential health issues associated with synthetic food color additives, the food industry has become particularly interested in replacing these additives with natural alternatives, including fruit and vegetable extracts.[1,2] Anthocyanins are a group of natural pigments responsible for the bright blue and red colors found in many flowers, fruits, and vegetables. They can be classified on the basis of the presence of hydrogen, hydroxyl, or methoxy substituents on the aglycone (Figure 1). Naturally, anthocyanidins are glycosylated with sugar moieties, including but not limited to glucoside, galactoside, sophoroside, rutinoside, and sambubioside, attached to the aglycone at the 3 -position for monoglycosides and the 3,5-positions for diglycosides.[3] Anthocyanins may also be acylated with the presence of moieties including phenolic acids such as ferulic, *p*-hydroxybenzoic, and caffeic acids on their glycosides.[4]

In addition to serving as potential natural alternatives to the synthetic color additives, anthocyanins have been reported to promote disease preventative properties. Reactive oxygen species are a concern to human health because of their ability to promote oxidative stress, age-related dysfunction, and damage to overall cardiovascular health.[5] Additionally, research has shown that dietary phytochemicals, including anthocyanins found in red wines, are capable of scavenging free radicals in vitro.[6,7] For instance, anthocyanins from fruits and vegetables including strawberries and grapes reduce the risk of neurodegenerative diseases by mitigating oxidative damage in cell culture models.[8,9]

Although promising as health-promoting natural colors, anthocyanins are susceptible to a diverse array of chemical reactions and are notoriously sensitive to heat, light, and oxygen. Thus, if anthocyanins are broadly applied in the replacement of synthetic food color additives, their stability to conditions of thermoprocessing, handling, and storage in the context of specific formulations must be investigated. Many previous studies focused on the degradation kinetics of anthocyanins in relation to their color, but not the anthocyanin compositions or concentrations.[10,11] Other studies examined the degradation kinetics of total monomeric anthocyanins in juices and concentrates.[12−14] However, few studies examined the total monomeric anthocyanin content and individual anthocyanin degradation kinetics in ready-to-drink (RTD) model beverages. Thermostress has been the focus of many of these studies, but there is a lack of publications concerning the degradation kinetics of anthocyanins through photostress and its implication on beverage shelf life. Furthermore, a significant portion of RTD beverages are acidified and either formulated with preservatives or thermally processed by high-temperature−short-time (HTST) treatment in both hot fill hold or aseptically filled. Fortification of RTD beverages with vitamins and minerals has also increased and may promote the degradation of anthocyanins. The objective of this study was therefore to determine the stability of anthocyanins in grape and purple sweet potato (PSP) extracts in multiple models of RTD beverages through photo- and thermostresses.

Received: October 15, 2012
Revised: January 17, 2013
Accepted: January 18, 2013
Published: January 18, 2013

dx.doi.org/10.1021/jf3044007 | *J. Agric. Food Chem.* 2013, 61, 1364−1372

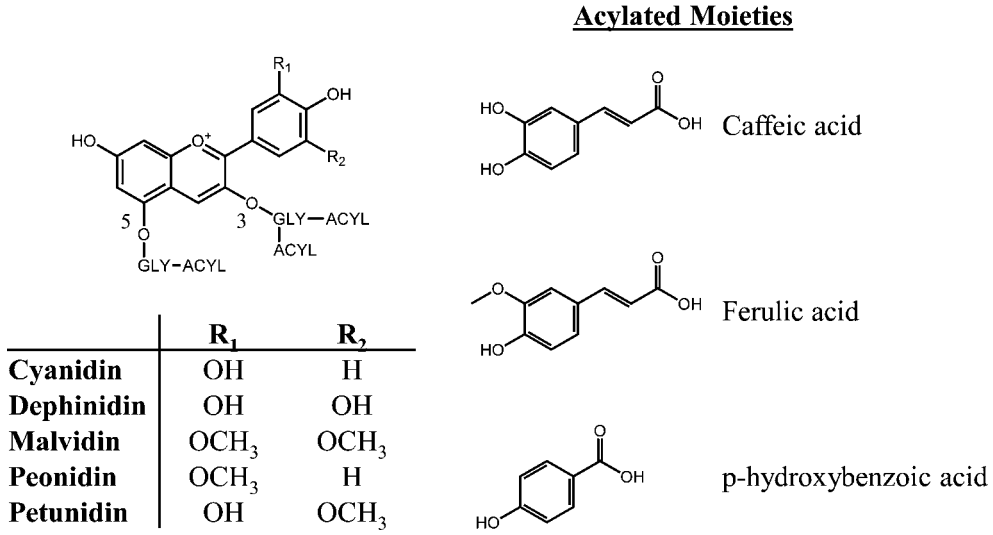

	R_1	R_2
Cyanidin	OH	H
Dephinidin	OH	OH
Malvidin	OCH_3	OCH_3
Peonidin	OCH_3	H
Petunidin	OH	OCH_3

Figure 1. Structures of anthocyanin backbones (left) and common acylated moieties (right) found in PSP extract. "GLY" (positions 3 and 5) and "ACYL" represent glycosides and acylated moieties, respectively.

MATERIALS AND METHODS

Materials. Ascorbic acid (AA), citric acid, sodium citrate, sodium benzoate, and potassium sorbate were obtained from Sigma-Aldrich (St. Louis, MO, USA). Formic acid, LC-MS grade water, acetonitrile, potassium chloride, hydrochloric acid, and sodium acetate were purchased from VWR (Radnor, PA, USA). Sensient Colors Inc. (St. Louis, MO, USA) graciously donated a model vitamin-enriched water premix powder, rubired grape, and purple sweet potato extracts. The vitamin-enriched water premix powder contained 25 mg, 0.83 mg, 0.17 mg, 0.25 μg, 0.83 mg, 0.62 mg, and 5 μg of vitamins C, B3, B6, B12, and B5, zinc(II), and chromium(III) in a 100 mL solution, respectively. Authentic standards of delphinidin, malvidin, cyanidin, petunidin, and peonidin glucosides were purchased from Chromadex Inc. (Irvine, CA, USA).

Model Beverages. Model RTD beverages were created to mimic typical compositions commonly used in the beverage industry. This included a vitamin-enriched water model beverage (pH 3.60 ± 0.02), a hot fill model beverage (pH 3.60 ± 0.02) with various AA concentrations, and a preserved model beverage (pH 3.00 ± 0.02) containing sodium benzoate and potassium sorbate. The vitamin-enriched water (VEW) model was formulated with 0.025% AA and 0.044% of a model vitamin water powdered premix in deionized water. Hot fill model beverages were formulated with 0.00, 0.01, or 0.05% AA and also contained 1.60% citric acid and 1.00% sodium citrate in deionized water. A preserved model beverage was formulated with 0.05% sodium benzoate, 0.01% potassium sorbate, 2% citric acid, and 0.60% sodium citrate in deionized water. Both rubired grape and PSP extracts were dosed into the VEW model beverage to illustrate the differences in extracts rich in acylated and nonacylated anthocyanins, respectively. Rubired grape was added into all other model beverages to evaluate the stability of nonacylated anthocyanins across all model beverages. Amounts of 0.11 and 0.04% of rubired grape and PSP extract were used throughout the experiments, respectively. Extract concentrations were selected on the basis of matching color profiles provided by Sensient Colors Ltd.

Photo- and Thermostresses. After each model beverage was created, an aliquot of each solution was transferred into clear borosilicate glass tubes, flushed with nitrogen, and hermetically sealed. Thermostress was induced by using a Precision Scientific Thelco (Chicago, IL, USA) water bath set at 40, 60, and 80 °C for all model beverages. Photostress was induced by using an Atlas Material Testing Technology LLC Suntest (Chicago, IL, USA) lightbox equipped with a xenon lamp at 250, 500, and 750 W/m^2 (equivalently 47.1, 95.1, and 143.1 klx, respectively). Vitamin-enriched water samples were retrieved at 0, 15, 30, 60, 120, 240, and 360 min of stress, whereas all other model beverages were retrieved at 0, 60, 120, 240, 360, 480, 600, 720, and 1440 min.

Anthocyanin Analysis. All beverage samples were analyzed for anthocyanin content by pH differential total monomeric anthocyanin content and LC-MS. The pH differential technique was used as described by Giusti et al.,[15] with minor volume modifications to fit a 96-well plate reader. Very briefly, 60 μL of each solution was transferred into two separate wells containing 0.24 mL of either 0.025 M potassium chloride buffer (pH 1.00) or 0.4 M sodium acetate buffer (pH 4.50). After incubation at room temperature for 15 min, their absorptions were recorded at 510 and 700 nm using a Molecular Devices Spectra Max 100 (Sunnyvale, CA, USA). Total monomeric anthocyanins were calculated on the basis of cyanidin 3-glucoside equivalents.

Prior to all LC-MS analyses, samples were prepared by solid phase extraction. Waters Oasis HLB 1 cm^3 cartridges (Milford, MA, USA) were prepared by sequentially rinsing with methanol and water. Model beverage samples were loaded onto each cartridge and rinsed with 2% formic acid in water. Anthocyanins were eluted with 2% formic acid in methanol. Samples were dried in a Labconco RapidVap (Kansis City, MO, USA) and solubilized in 200 μL of 95:5 mobile phases A and B.

Samples were injected in a Waters 2695 separations module equipped with a Waters Xterra reverse phase C18 3.5 μm 2.1 × 100 mm column in a heated chamber set at 35 °C. A linear biphasic gradient with a flow rate of 0.30 mL/min with mobile phase A, 2% formic acid in MS grade water, and mobile phase B, 0.1% formic acid in acetonitrile. At 0, 10, 30, and 31 min, the solvent composition was 95, 90, 75, and 95% mobile phase A. Directly tandem to the column, the flow was split so that half of it went to a Waters 2996 photodiode array detector and half to a Waters Micromass ZQ mass spectrometer. Positive mode electrospray ionization was used with capillary, cone, and extractor voltages set to 2500, 50, and 3 V, respectively. Source and desolvation temperatures were set to 150 and 300 °C, respectively. Nitrogen gas cone and desolvation flow rates were set to 25 and 250 L/h, respectively. Single ion responses were set to m/z 303.8, 331.7, 287.5, 317.7, and 301.7 to detect delphinidin, malvidin, cyanidin, petunidin, and peonidin, respectively.

Acylated anthocyanins were identified and analyzed by a LC-time-of-flight (TOF) MS. Samples were injected into a Hewlett-Packard series 1100 LC system (Palo Alto, CA, USA) connected to a Waters LCT Premier. The LC-MS method, column, and MS conditions were identical to what was previously described for the Waters 2695 separations module. However, the cone voltages varied from 30, 50, and 70 V to fragment acylated anthocyanins and aid in identification.

Kinetic Models. Previous studies have shown that anthocyanins typically follow first-order kinetics and Arrhenius behavior through

dx.doi.org/10.1021/jf3044007 | J. Agric. Food Chem. 2013, 61, 1364−1372

thermostress.[12−14,16] Reaction rate constants for both total monomeric and individual anthocyanins were calculated by creating a plot of the natural log of anthocyanin concentration at a given time (C) divided by the initial anthocyanin concentration (C_0) as a function of treatment time (Figures 3 and 4). Furthermore, activation energies (E_a) for thermotreatments were calculated by solving for $-E_a/R$ via a linear plot of the natural log of each degradation rate versus inverse temperature.

Experimental Design and Statistical Analysis. The study was split into four different experiments, two focused on the degradation rates of total monomeric anthocyanins and the others focused on the degradation rates of individual anthocyanins. Within each set experiments, they were further segregated by their exposure to either thermo- or photostress. Correlations between photo- and thermostress groups would be particularly difficult to interpret given that their degradation mechanisms are different. The total monomeric anthocyanin degradation rate experiments followed a 3 × 5 factorial design, where three intensity levels of thermo/phototreatment were selected for all five model beverages. Similarly, individual anthocyanin degradation rate experiments followed a 3 × 5 × 5 design, where five individual anthocyanidin glucosides are additional variables. Degradation rate constants are expressed as the mean ± the standard error of the mean. Group differences within each experiment were determined by analysis of variance and Tukey's test (α = 0.05) using Statistical Analysis Systems 9.2 (SAS Institute, Cary, NC, USA). Each model beverage was run as triplicates for each of the photo- and thermoconditions.

RESULTS AND DISCUSSION

Anthocyanin Profiles. Qualitative and quantitative anthocyanin profiles of grape and PSP extracts were noticeably different. Total monomeric anthocyanin concentrations were 26.44 and 15.64 cyanidin 3-*O*-glucoside equivalents g/L in grape and PSP extracts, respectively. Chromatograms for both grape and PSP corresponding to each aglycone m/z were analyzed (Figure 2). Grape extract primarily consisted of

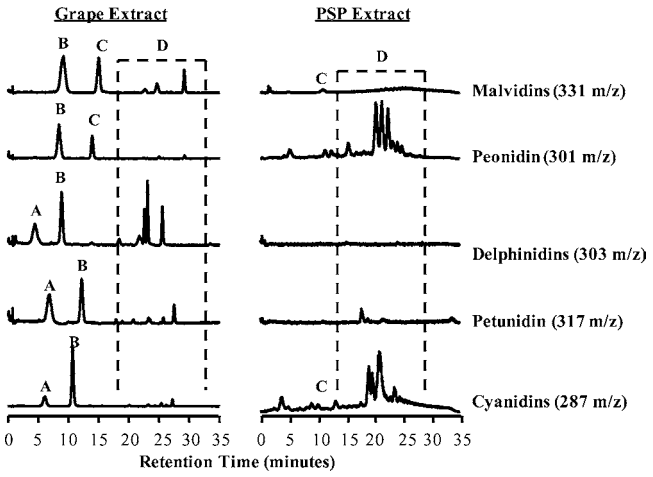

Figure 2. Normalized extracted ion chromatograms for grape and PSP extracts. Peaks labeled A−D correspond to 3,5-diglucosides, 3-*O*-glucosides, unidentified anthocyanins, and acylated anthocyanins, respectively, of each of the indicated aglycone chromatograms.

nonacylated 3-*O*-glucosides of delphinidin, malvidin, cyanidin, petunidin, and peonidin. In contrast, PSP extract primarily contained mono- and diacylated 3-sophoroside-5-glucosides of peonidin and cyanidins (Table 1).

Impact of Thermostress on Grape Anthocyanin Degradation Rates. The total monomeric anthocyanin degradation rates for model beverages containing grape extract

Table 1. Major Anthocyanin Species Present in Grape and PSP Extracts[a]

Grape Extract			
compound	rel concn (%)	parent ion (m/z)	fragment (m/z)
malvidin 3-*O*-glucoside	25.8	493	331
peonidin 3-*O*-glucoside	9.8	463	301
delphinidin 3,5-diglucoside	3.1	627	303
delphinidin 3-*O*-glucoside	2.2	465	303
petunidin 3,5-diglucoside	3.5	641	317
petunidin 3-*O*-glucoside	1.7	479	317
cyanidin 3,5-diglucoside	8.9	611	287
cyanidin 3-*O*-glucoside	17.1	449	287
PSP Extract			
tentative identification	rel concn (%)	parent ion (m/z)	fragment (m/z)
peonidin-3-dicaffeoylsophoroside-5-glucoside	12.1	1111	949, 463, 301
peonidin-3-caffeoyl-*p*-hydroxybenzoylsophoroside-5-glucoside	18.5	1069	907, 787, 625, 463, 301
peonidin-3-caffeoylferuloylsophoroside-5-glucoside	14.5	1125	963, 463, 301
peonidin-3-caffeoylsophoroside-5-glucoside	6.3	949	787, 463, 301
peonidin-3-*p*-hydroxybenzoylsophoroside-5-glucoside	3.7	907	301
peonidin-3-feruloylsophoroside-5-glucoside	2.5	963	301
total acylated cyanidin-3-sophoroside-5-glucosides	34.5		611, 449, 287

[a]Relative concentrations (rel concn) are represented as moles of anthocyanin/total anthocyanin moles in each extract. Identities of glucosides in grape extracts were confirmed by analytical standards and mass spectroscopy. Tentative identifications were based on previous studies on PSP acylated anthocyanins, parent ions, and fragment ions.[4,30].

at 80 °C were significantly greater that of either 40 or 60 °C treatment (Table 2). For example, the degradation rates were 3.38×10^{-4}, 4.84×10^{-4}, and 1.00×10^{-3} min^{-1} at 40, 60, and 80 °C when incubated in the 500 ppm AA hot fill model beverage, respectively. As previously mentioned, anthocyanin degradation typically follows first-order kinetics and Arrhenius behavior, which is likely to be responsible for this observation. Kechinski et al. previously reported that total monomeric anthocyanin content in blueberry juice had very similar degradation rates of 6.40×10^{-5}, 4.57×10^{-4}, and 2.25×10^{-3} min^{-1} at 40, 60, and 80 °C, respectively.[13] Furthermore, the increase in thermotreatment resulted in similar significant differences for all anthocyanidin 3-*O*-glucosides in the grape extract (Table 3). Delphinidin, malvidin, petunidin, peonidin, and cyanidin 3-*O*-glucosides are predominant anthocyanin species in the grape extract. Thus, the degradation rates for both total monomeric anthocyanins and anthocyanidin 3-*O*-glucosides are likely to follow similar significant differences across thermotreatments.

Interestingly, negative values for degradation rates were calculated for individual anthocyanins in the 0 ppm AA hot fill and preserved model beverages (Table 3). Although this may imply that these anthocyanidin 3-*O*-glucosides are increasing in concentration, this is highly unlikely given the conditions of

Table 2. Total Monomeric Anthocyanin Degradation Rates and Activation Energies under Thermostress[a]

model beverage	40 °C (min^{-1})	°60 C (min^{-1})	80 °C (min^{-1})	E_a (kJ/mol)
0 ppm AA hot fill	$1.36 \times 10^{-5} \pm 4.8 \times 10^{-5}$ ^{1A}	$1.71 \times 10^{-4} \pm 3.3 \times 10^{-5}$ ^{2A}	$9.43 \times 10^{-4} \pm 1.2 \times 10^{-5}$ ^{3A}	60.48 ± 3.3 ^{AB}
100 ppm AA hot fill	$3.34 \times 10^{-4} \pm 3.9 \times 10^{-5}$ ^{1B}	$3.32 \times 10^{-4} \pm 6.9 \times 10^{-5}$ ^{1AB}	$9.69 \times 10^{-4} \pm 2.3 \times 10^{-5}$ ^{2A}	24.20 ± 2.8 ^{C}
500 ppm AA hot fill	$3.38 \times 10^{-4} \pm 2.0 \times 10^{-5}$ ^{1B}	$4.84 \times 10^{-4} \pm 6.5 \times 10^{-5}$ ^{1B}	$1.00 \times 10^{-3} \pm 2.0 \times 10^{-5}$ ^{2A}	24.78 ± 1.8 ^{C}
VEW (grape)	$3.02 \times 10^{-4} \pm 1.1 \times 10^{-5}$ ^{1B}	$5.02 \times 10^{-4} \pm 2.9 \times 10^{-5}$ ^{1B}	$1.88 \times 10^{-3} \pm 6.1 \times 10^{-5}$ ^{2B}	41.60 ± 0.2 ^{BC}
preserved model	$2.41 \times 10^{-5} \pm 2.4 \times 10^{-5}$ ^{1A}	$1.59 \times 10^{-4} \pm 2.2 \times 10^{-5}$ ^{1A}	$1.10 \times 10^{-3} \pm 8.6 \times 10^{-5}$ ^{2A}	80.07 ± 8.6 ^{A}

[a]Ascorbic acid and vitamin-enriched water are abbreviated AA and VEW, respectively. VEW (PSP) total monomeric anthocyanin degradation rates are not shown because of their deviation from first-order kinetics. All model beverages contained grape extract. VEW model beverage (pH 3.60 ± 0.02) contained 0.025% AA and 0.044% vitamin water powdered premix. All hot-filled model beverages (pH 3.60 ± 0.02) contained 0.60% citric acid and 1.00% sodium citrate, with various concentrations of AA indicated in the table. Preserved model beverage (pH 3.00 ± 0.02) contained 0.05% sodium benzoate, 0.01% potassium sorbate, 2% citric acid, and 0.60% sodium citrate. Different bold superscript numbers indicate significant differences ($P < 0.05$) between temperatures within each model beverage. Different bold superscript letters indicate significant differences ($P < 0.05$) between model beverages within each temperature or activation energy.

Table 3. Grape Anthocyanin Degradation Rates and Activation Energies under Thermostress[a]

	40 °C (min^{-1})	60 °C (min^{-1})	80 °C (min^{-1})	E_a (kJ/mol)
0 ppm AA Hot Fill				
delphinidin 3-*O*-glucoside	$2.18 \times 10^{-4} \pm 2.3 \times 10^{-4}$ $^{1A\alpha}$	$8.82 \times 10^{-4} \pm 8.3 \times 10^{-5}$ $^{1A\alpha}$	$1.89 \times 10^{-3} \pm 1.0 \times 10^{-4}$ $^{2A\alpha}$	30.29 ± 1.1 $^{A\alpha}$
malvidin 3-*O*-glucoside	$-4.50 \times 10^{-5} \pm 1.0 \times 10^{-4}$ $^{1A\alpha}$	$1.87 \times 10^{-4} \pm 6.6 \times 10^{-5}$ $^{1A\alpha}$	$1.51 \times 10^{-3} \pm 6.4 \times 10^{-5}$ $^{2A\alpha}$	67.52 ± 0.6 $^{B\alpha}$
petunidin 3-*O*-glucoside	$-1.65 \times 10^{-5} \pm 7.4 \times 10^{-5}$ $^{1A\alpha}$	$2.21 \times 10^{-4} \pm 5.2 \times 10^{-5}$ $^{1A\alpha}$	$1.42 \times 10^{-3} \pm 3.9 \times 10^{-4}$ $^{2A\alpha}$	65.77 ± 6.7 $^{B\alpha}$
peonidin 3-*O*-glucoside	$-3.67 \times 10^{-5} \pm 1.1 \times 10^{-4}$ $^{1A\alpha}$	$1.93 \times 10^{-4} \pm 4.7 \times 10^{-5}$ $^{1A\alpha}$	$1.31 \times 10^{-3} \pm 3.7 \times 10^{-5}$ $^{2A\alpha}$	59.97 ± 0.4 $^{B\alpha}$
cyanidin 3-*O*-glucoside	$1.65 \times 10^{-5} \pm 3.6 \times 10^{-5}$ $^{1A\alpha}$	$3.36 \times 10^{-4} \pm 9.1 \times 10^{-6}$ $^{1A\alpha}$	$1.64 \times 10^{-3} \pm 5.3 \times 10^{-5}$ $^{2A\alpha}$	75.71 ± 0.7 $^{B\alpha}$
100 ppm AA Hot Fill				
delphinidin 3-*O*-glucoside	$3.04 \times 10^{-4} \pm 1.6 \times 10^{-4}$ $^{1A\alpha}$	$6.49 \times 10^{-4} \pm 2.7 \times 10^{-5}$ $^{1A\alpha}$	$1.54 \times 10^{-3} \pm 1.9 \times 10^{-4}$ $^{2A\alpha}$	43.12 ± 11.7 $^{A\alpha}$
malvidin 3-*O*-glucoside	$3.51 \times 10^{-4} \pm 6.9 \times 10^{-6}$ $^{1A\alpha\beta}$	$2.74 \times 10^{-4} \pm 2.1 \times 10^{-5}$ $^{1A\alpha}$	$1.31 \times 10^{-3} \pm 1.4 \times 10^{-4}$ $^{2A\alpha}$	29.19 ± 3.0 $^{A\beta}$
petunidin 3-*O*-glucoside	$3.51 \times 10^{-4} \pm 9.7 \times 10^{-5}$ $^{1A\alpha\beta}$	$2.99 \times 10^{-4} \pm 1.1 \times 10^{-5}$ $^{1A\alpha}$	$1.53 \times 10^{-3} \pm 1.7 \times 10^{-4}$ $^{2A\alpha}$	34.12 ± 4.1 $^{A\beta}$
peonidin 3-*O*-glucoside	$3.13 \times 10^{-4} \pm 8.4 \times 10^{-5}$ $^{1A\alpha\beta}$	$1.68 \times 10^{-4} \pm 9.4 \times 10^{-6}$ $^{1A\alpha}$	$1.11 \times 10^{-3} \pm 2.2 \times 10^{-4}$ $^{2A\alpha}$	28.58 ± 1.9 $^{A\beta}$
cyanidin 3-*O*-glucoside	$3.61 \times 10^{-4} \pm 2.1 \times 10^{-5}$ $^{1A\alpha\beta}$	$3.81 \times 10^{-4} \pm 1.3 \times 10^{-6}$ $^{1A\alpha}$	$1.47 \times 10^{-3} \pm 1.6 \times 10^{-4}$ $^{2A\alpha}$	31.49 ± 3.9 $^{A\beta}$
500 ppm AA Hot Fill				
delphinidin 3-*O*-glucoside	$6.83 \times 10^{-4} \pm 1.5 \times 10^{-5}$ $^{1A\alpha}$	$1.11 \times 10^{-3} \pm 5.8 \times 10^{-5}$ $^{1A\alpha}$	$1.70 \times 10^{-3} \pm 4.9 \times 10^{-5}$ $^{2A\alpha}$	20.93 ± 1.2 $^{A\alpha}$
malvidin 3-*O*-glucoside	$5.16 \times 10^{-4} \pm 4.9 \times 10^{-5}$ $^{1A\alpha\beta}$	$7.44 \times 10^{-4} \pm 1.1 \times 10^{-4}$ $^{1A\alpha\beta}$	$1.23 \times 10^{-3} \pm 1.3 \times 10^{-4}$ $^{2A\alpha}$	19.89 ± 0.4 $^{A\beta}$
petunidin 3-*O*-glucoside	$5.96 \times 10^{-4} \pm 2.9 \times 10^{-5}$ $^{1A\alpha\beta}$	$8.92 \times 10^{-4} \pm 9.4 \times 10^{-5}$ $^{1A\alpha\beta}$	$1.69 \times 10^{-3} \pm 6.0 \times 10^{-5}$ $^{2A\alpha}$	23.81 ± 1.8 $^{A\beta}$
peonidin 3-*O*-glucoside	$5.42 \times 10^{-4} \pm 5.1 \times 10^{-5}$ $^{1A\alpha\beta}$	$7.94 \times 10^{-4} \pm 9.2 \times 10^{-5}$ $^{1A\alpha\beta}$	$1.40 \times 10^{-3} \pm 3.9 \times 10^{-5}$ $^{2A\alpha}$	21.84 ± 2.7 $^{A\beta}$
cyanidin 3-*O*-glucoside	$6.64 \times 10^{-4} \pm 1.2 \times 10^{-5}$ $^{1A\beta}$	$9.57 \times 10^{-4} \pm 7.9 \times 10^{-5}$ $^{1A\beta}$	$1.62 \times 10^{-3} \pm 4.6 \times 10^{-5}$ $^{2A\alpha}$	20.43 ± 1.0 $^{A\beta}$
Vitamin-Enriched Water				
delphinidin 3-*O*-glucoside	$5.04 \times 10^{-4} \pm 5.7 \times 10^{-4}$ $^{1A\alpha}$	$1.36 \times 10^{-3} \pm 3.8 \times 10^{-4}$ $^{1A\alpha}$	$4.57 \times 10^{-3} \pm 2.9 \times 10^{-4}$ $^{2A\beta}$	29.91 ± 1.2 $^{A\alpha}$
malvidin 3-*O*-glucoside	$7.70 \times 10^{-4} \pm 2.3 \times 10^{-4}$ $^{1A\beta}$	$1.06 \times 10^{-3} \pm 8.9 \times 10^{-5}$ $^{1A\beta}$	$3.21 \times 10^{-3} \pm 7.1 \times 10^{-5}$ $^{2A\beta}$	34.09 ± 6.9 $^{A\beta}$
petunidin 3-*O*-glucoside	$1.03 \times 10^{-3} \pm 1.8 \times 10^{-4}$ $^{1A\beta}$	$1.28 \times 10^{-3} \pm 1.4 \times 10^{-5}$ $^{1A\beta}$	$4.01 \times 10^{-3} \pm 1.8 \times 10^{-4}$ $^{2A\beta}$	31.15 ± 3.0 $^{A\beta}$
peonidin 3-*O*-glucoside	$7.87 \times 10^{-4} \pm 2.3 \times 10^{-4}$ $^{1A\beta}$	$1.14 \times 10^{-3} \pm 5.4 \times 10^{-5}$ $^{1A\beta}$	$3.81 \times 10^{-3} \pm 1.6 \times 10^{-4}$ $^{2A\beta}$	37.34 ± 6.2 $^{A\beta}$
cyanidin 3-*O*-glucoside	$1.08 \times 10^{-3} \pm 5.7 \times 10^{-5}$ $^{1A\delta}$	$1.30 \times 10^{-3} \pm 4.0 \times 10^{-5}$ $^{1A\beta}$	$4.55 \times 10^{-3} \pm 5.5 \times 10^{-5}$ $^{2A\beta}$	26.89 ± 0.7 $^{A\beta}$
Preserved Model				
delphinidin 3-*O*-glucoside	$-1.48 \times 10^{-5} \pm 7.8 \times 10^{-5}$ $^{1A\alpha}$	$1.57 \times 10^{-4} \pm 8.1 \times 10^{-6}$ $^{1A\alpha}$	$2.25 \times 10^{-3} \pm 1.2 \times 10^{-4}$ $^{2A\alpha}$	75.39 ± 1.3 $^{A\beta}$
malvidin 3-*O*-glucoside	$-5.35 \times 10^{-5} \pm 8.4 \times 10^{-5}$ $^{1A\alpha}$	$7.67 \times 10^{-5} \pm 1.8 \times 10^{-5}$ $^{1A\alpha}$	$9.37 \times 10^{-4} \pm 3.1 \times 10^{-6}$ $^{2A\alpha}$	66.37 ± 0.1 $^{A\alpha}$
petunidin 3-*O*-glucoside	$-1.69 \times 10^{-5} \pm 9.8 \times 10^{-5}$ $^{1A\alpha}$	$1.53 \times 10^{-4} \pm 2.4 \times 10^{-5}$ $^{1A\alpha}$	$1.35 \times 10^{-3} \pm 6.6 \times 10^{-5}$ $^{2A\alpha}$	58.09 ± 1.3 $^{A\alpha}$
peonidin 3-*O*-glucoside	$-5.16 \times 10^{-5} \pm 9.1 \times 10^{-5}$ $^{1A\alpha}$	$8.23 \times 10^{-5} \pm 2.1 \times 10^{-5}$ $^{1A\delta}$	$9.16 \times 10^{-4} \pm 8.2 \times 10^{-5}$ $^{2A\alpha}$	60.88 ± 2.0 $^{A\alpha}$
cyanidin 3-*O*-glucoside	$-1.76 \times 10^{-5} \pm 6.0 \times 10^{-5}$ $^{1A\alpha}$	$8.03 \times 10^{-5} \pm 4.6 \times 10^{-5}$ $^{1A\alpha}$	$1.03 \times 10^{-3} \pm 7.2 \times 10^{-5}$ $^{2A\delta}$	65.18 ± 0.9 $^{A\alpha}$

[a]VEW model beverage (pH 3.60 ± 0.02) contained 0.025% ascorbic acid (AA) and 0.044% vitamin water powdered premix. All hot filled model beverages (pH 3.60 ± 0.02) contained 0.60% citric acid and 1.00% sodium citrate, with various concentrations of AA indicated in the table. Preserved model beverage (pH 3.00 ± 0.02) contained 0.05% sodium benzoate, 0.01% potassium sorbate, 2% citric acid, and 0.60% sodium citrate. Different bold superscript numbers indicate significant differences ($P < 0.05$) between temperatures within each model beverage and anthocyanin. Different bold superscript Roman letters indicate significant differences ($P < 0.05$) between anthocyanins within each temperature and model beverage. Different bold superscript Greek letters indicate significant differences ($P < 0.05$) between model beverages within each temperature and anthocyanin.

these experiments. Negative degradation rates were only observed in the most stable model beverages coupled with the mildest thermotreatment, suggesting only minimal changes to anthocyanin content. Furthermore, negative values were only obtained when the absolute value of the mean was less than the standard error of the mean (Table 3). This is likely due to the inability of the LC-MS analysis of individual anthocyanins to distinguish the extremely low degradation from analytical noise. However, because the pH differential method measures total monomeric anthocyanins, it was more capable of assessing broad changes in the degradation of total anthocyanins throughout the thermotreatment.

Impact of Model Beverages on Anthocyanin Degradation Rates through Thermostress. Increasing concen-

trations of AA had various impacts on total monomeric anthocyanin degradation rates (Table 2). At 40 °C, degradation rates significantly increased from 1.36×10^{-5} to 3.34×10^{-4} min^{-1} with the addition of 100 ppm AA. However, the further addition of 400 ppm AA caused no significant increase in the degradation rate. At 60 °C there was only a significant increase in degradation rates between 0 and 500 ppm AA and no significant difference at 80 °C for any of the three hot fill model beverages. Like anthocyanins, AA is vulnerable to high temperatures and may rapidly degrade in the model beverages.[17] Thus, the specific effect of AA on anthocyanin degradation may diminish at elevated temperatures. Therefore, AA caused significant differences in anthocyanin degradation rates only at low temperatures, and its effect became more negligible at higher temperatures. Previous studies have shown that the addition of AA reduces anthocyanin stability at lower temperatures. For instance, Calvi and Francis found that the addition of AA to model beverages increased the rates of degradation at 37.7, 23.8, and 1.1 °C.[18] However, unlike the present study, they did not investigate the diminishing effect of AA on anthocyanin degradation at elevated temperatures including 60 and 80 °C. Many beverages are exposed to high temperatures during processing; thus, the interaction between temperature, AA concentration, and anthocyanin degradation must be considered in beverage production.

Varying AA concentrations between hot fill model beverages did not significantly increase most anthocyanidin 3-*O*-glucoside degradation rates at a given temperature (Table 3). The only exception was cyanidin 3-*O*-glucoside, for which the degradation rate significantly increased from 1.65×10^{-5} to 6.64×10^{-4} min^{-1} and from 3.36×10^{-4} to 9.57×10^{-4} min^{-1} with the addition of 500 ppm AA at 40 and 60 °C, respectively. Cyanidin 3-*O*-glucoside is particularly sensitive to AA relative to the other anthocyanidin 3-*O*-glucosides present in the grape extract. Therefore, the significant increase in total monomeric anthocyanin degradation rates discussed previously may have been predominantly driven by cyanidin 3-*O*-glucoside. Talcott et al. examined the effect of the addition of 800 ppm AA on red muscadine grape anthocyanin 3,5-diglucosides through pasteurization (95 °C for 15 min).[19] In contrast to our findings, anthocyanidins had a significant impact on anthocyanidin 3,5-diglucoside stability. For instance, significant differences were observed for cyanidin, pelargonin, peonidin, and malvidin 3,5-diglucosides, but not for delphinidin and petunidin 3,5-diglucoside. It is likely that 800 ppm AA was concentrated enough to significantly affect most anthocyanin degradation rates, whereas 500 ppm was enough to cause only particularly sensitive anthocyanins to significantly reduce stability.

There was no significant difference in total monomeric degradation rates between the VEW and the 500 ppm AA model beverages at 40 and 60 °C. However, the VEW had a significantly greater degradation rate at 80 °C (Table 2). Similarly, degradation rates for all anthocyanidin 3-*O*-glucosides were significantly greater in the VEW than the 500 ppm AA model beverage at 80 °C (Table 3). It is likely that the increase in degradation rates is caused by the presence of metal ions and B vitamins in the VEW premix. Zinc(II) and chromium(III), which are present in the VEW model beverage, may act as oxidizing agents and may have contributed to anthocyanin oxidation, leading to more rapid degradation. B vitamins are typically thermally stable, and their interactions with anthocyanins have yet to be explored individually. Complex model beverages and juices contain many different compounds, and anthocyanin degradation rates are particularly difficult to compare between studies. Thus, further research is required to determine the impact of the food ingredients on anthocyanin degradation.

Arrhenius Behavior and Activation Energies. The exponential increase in degradation rates with elevated temperatures is typical of Arrhenius behavior and has been reported in several other studies.[12−14,16] Activation energies for the degradation of total monomeric anthocyanins were calculated for each solution (Table 2). The 0 ppm AA and preserved model beverages had the greatest activation energies at 60.48 and 80.07 kJ/mol, respectively, indicating that they are the most resilient to thermostress. Dybry et al. investigated grape skin anthocyanin stability in a pH 3.0 buffer and calculated an activation energy of 58 kJ/mol.[20] This is in agreement with the activation energy of the 0 ppm AA hot fill model beverage (pH 3.6) used in this study. Furthermore, the addition of at least 100 ppm AA significantly reduced the activation energy to 24.20 kJ/mol. However, an additional 400 ppm did not significantly alter the activation energy. Therefore, AA concentrations of at least 100 ppm in a beverage will significantly reduce the anthocyanin degradation activation energy and thus change the response of the degradation rates between temperatures. Additional studies are required to investigate the change in activation energies with the addition of AA at concentrations lower than 100 ppm. Multiple mechanisms for degradative reactions between ascorbic acid and anthocyanins have been hypothesized. One mechanism involved the formation of reactive oxygen species, such as peroxide, from the oxidation of ascorbic acid and their subsequent reaction with anthocyanins.[21,22] Another proposed mechanism involves a condensation reaction between ascorbic acid and anthocyanins.[23] Although products of individual anthocyanin−ascorbic acid condensation were not observed in the present study, it is important to highlight that the analytical conditions applied were likely not optimized for these analyses. Therefore, it remains unclear which reactions may predominate in the model beverages and conditions investigated in the present study. Additional studies into the specific mechanisms are therefore warranted.

Typically, activation energies of the anthocyanins were not significantly different in each model beverage (Table 3). A study by Attoe and Von Elbe found no significant difference between the activation energies of cyanidin and peonidin 3-arabinosides and 3-galatosides in a pH 2.5 buffer during dark conditions.[24] However, in the present study, delphinidin 3-*O*-glucoside in the 0 ppm AA hot fill model was the only exception and had a significantly lower activation energy of 30.29 kJ/mol in comparison with all other anthocyanins, indicating that it is the most sensitive to temperature changes. Additionally, delphinidin 3-*O*-glucoside had no significant change in activation energy with the addition of ascorbic acid or vitamin premix. However, in the preserved base, delphinidin 3-*O*-glucoside activation energy significantly increased to 75.39 kJ/mol, highlighting the stability of the preserved base. Activation energies of malvidin, petunidin, peonidin, and cyanidin 3-*O*-glucosides significantly decreased with the addition of 100 ppm AA, but not with an additional 400 ppm AA. For instance, in the 0, 100, and 500 ppm AA bases, cyanidin 3-*O*-glucoside had activation energies of 75.71, 31.49, and 20.43 kJ/mol, respectively. These observations agree with the significant differences in total monomeric anthocyanin degradation activation energies and provide further evidence for

the impact of AA on anthocyanin stability through thermostress.

Grape and Purple Sweet Potato Anthocyanins under Thermostress. Total monomeric anthocyanin degradation rates of PSP and grape extracts under thermostress could not be compared. It has been well documented that the total monomeric anthocyanin degradation of grape extract follows first-order kinetics. However, extracts containing relatively high concentrations of acylated anthocyanins, such as PSP, do not fit a first-order degradation model through short-term thermotreatments (Figure 3).[20,25] Correlation coefficients for PSP extract in the VEW model were 0.24, 0.06, and 0.14 at 40, 60, and 80 °C, respectively. Our results agree with previous short-term thermostability studies on acylated anthocyanin-rich extracts. For example, degradation rates for red cabbage extract in a soft drink system could be measured only after 6 h at 80 °C.[20] However, it is generally accepted that acylated anthocyanins are more stable than nonacylated anthocyanins through thermostress because of the protection of the flavylium cation through intramolecular copigmentation interactions.[26]

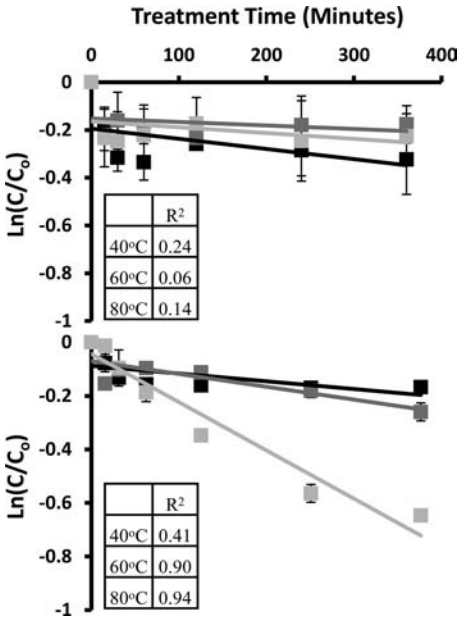

Figure 3. Total monomeric anthocyanin first-order kinetic plots for PSP (top) and grape (bottom) in VEW model beverages during thermotreatment. Black, dark gray, and light gray squares correspond to 40, 60, and 80 °C treatments, respectively. "C" and "C_0" are the total monomeric anthocyanin concentrations at a given time and the initial time, respectively.

Impact of Model Beverages on Anthocyanin Degradation Rates through Photostress. With the exception of the preserved model beverage, high intensities of photostress yielded greater total monomeric anthocyanin degradation rates (Table 4). The decreased pH of the preserved base is likely to be responsible, in part, for this observation. The stability of anthocyanins has previously been shown to increase with decreasing pH.[27] Between 250 and 500 W/m^2 treatments, degradation rates significantly increased from 6.26×10^{-4} to 2.73×10^{-3} and from 6.76×10^{-4} to 1.58×10^{-3} min^{-1} in 0 and 100 ppm AA model beverages, respectively. Additionally, total monomeric anthocyanin degradation rates significantly increased in the 500 ppm AA and VEW model beverages from 6.16×10^{-4} to 1.54×10^{-3} min^{-1} and from 6.45×10^{-4} to 1.85×10^{-3} min^{-1} at 250 and 750 W/m^2, respectively. Furthermore, most anthocyanidin 3-*O*-glucosides followed the same significant differences as the total monomeric anthocyanin degradation rates, providing further evidence of their similar susceptibilities to photostress (Table 5).

At 250 W/m^2, the total monomeric anthocyanin degradation rates in any of the model beverage bases were not significantly different. This may be attributed to the relatively low magnitude of photostress and treatment time. Significant differences may be observed at lower light intensities at extended incubation times; however, that was not investigated in the present study. In contrast, at 500 and 750 W/m^2, the addition of at least 100 ppm AA significantly decreased the total monomeric anthocyanin degradation rates (Table 4). For example, the addition of 100 ppm AA caused the degradation rate to significantly decrease from 2.73×10^{-3} to 1.58×10^{-3} min^{-1} during the 500 W/m^2 photostress treatment. Similarly, anthocyanidin 3-*O*-glucosides in the 0 ppm AA model beverage had significantly greater degradation rates than those in the 100 and 500 ppm AA bases at 500 and 750 W/m^2, but not 250 W/m^2 (Table 5). In contrast to thermostress, increased concentrations of AA protected anthocyanins from photostress. Typically, the presence of AA has been associated with the rapid degradation of anthocyanins in beverage systems. Our results clearly demonstrate that AA can have various effects depending on whether thermo- or photostresses are the major concern.

Grape and Purple Sweet Potato Anthocyanins under Photostress. In contrast to thermotreatments, the total

Table 4. Total Monomeric Anthocyanin Degradation Rates and Activation Energies under Photostress[a]

model beverage	250 W/m^2 (min^{-1})	500 W/m^2 (min^{-1})	750 W/m^2 (min^{-1})
0 ppm AA hot fill	$6.26 \times 10^{-4} \pm 8.6 \times 10^{-5}$ **1A**	$2.73 \times 10^{-3} \pm 9.7 \times 10^{-5}$ **2A**	$3.59 \times 10^{-3} \pm 2.1 \times 10^{-4}$ **3A**
100 ppm AA hot fill	$6.76 \times 10^{-4} \pm 2.7 \times 10^{-5}$ **1A**	$1.58 \times 10^{-3} \pm 1.5 \times 10^{-4}$ **2BC**	$1.45 \times 10^{-3} \pm 1.1 \times 10^{-4}$ **2BC**
500 ppm AA hot fill	$6.16 \times 10^{-4} \pm 4.9 \times 10^{-5}$ **1A**	$1.16 \times 10^{-3} \pm 1.0 \times 10^{-4}$ **12BD**	$1.54 \times 10^{-3} \pm 1.4 \times 10^{-4}$ **2BC**
VEW (grape)	$6.45 \times 10^{-4} \pm 7.7 \times 10^{-5}$ **1A**	$1.00 \times 10^{-3} \pm 2.2 \times 10^{-5}$ **1BD**	$1.85 \times 10^{-3} \pm 1.0 \times 10^{-4}$ **2BD**
VEW (PSP)	$1.29 \times 10^{-3} \pm 3.3 \times 10^{-5}$ **1B**	$2.02 \times 10^{-3} \pm 2.6 \times 10^{-5}$ **2C**	$2.40 \times 10^{-3} \pm 1.9 \times 10^{-4}$ **2AD**
preserved model	$7.33 \times 10^{-4} \pm 1.2 \times 10^{-4}$ **1A**	$9.20 \times 10^{-4} \pm 5.4 \times 10^{-5}$ **1D**	$1.16 \times 10^{-3} \pm 8.2 \times 10^{-5}$ **1C**

[a]Purple sweet potato extract, ascorbic acid, and vitamin-enriched water are abbreviated PSP, AA, and VEW, respectively. VEW contained either PSP or grape extract, whereas all other model beverages contained grape extract. VEW model beverage (pH 3.60 ± 0.02) contained 0.025% AA and 0.044% vitamin water powdered premix. All hot filled model beverages (pH 3.60 ± 0.02) contained 0.60% citric acid and 1.00% sodium citrate, with various concentrations of AA indicated in the table. Preserved model beverage (pH 3.00 ± 0.02) contained 0.05% sodium benzoate, 0.01% potassium sorbate, 2% citric acid, and 0.60% sodium citrate. Different bold superscript numbers indicate significant differences ($P < 0.05$) between light intensity within each model beverage. Different bold superscript letters indicate significant differences ($P < 0.05$) between model beverages within each light intensity.

Table 5. Grape Anthocyanin Degradation Rates under Photostress[a]

	250 W/m^2 (min^{-1})	500 W/m^2 (min^{-1})	750 W/m^2 (min^{-1})
0 ppm AA Hot Fill			
delphinidin 3-*O*-glucoside	$1.51 \times 10^{-3} \pm 2.3 \times 10^{-4}$ $^{1A\alpha}$	$9.12 \times 10^{-3} \pm 1.2 \times 10^{-3}$ $^{2A\alpha}$	$1.02 \times 10^{-2} \pm 2.1 \times 10^{-3}$ $^{2A\alpha}$
malvidin 3-*O*-glucoside	$5.68 \times 10^{-4} \pm 3.2 \times 10^{-5}$ $^{1A\alpha}$	$5.92 \times 10^{-3} \pm 3.6 \times 10^{-4}$ $^{2A\alpha}$	$5.56 \times 10^{-3} \pm 1.2 \times 10^{-4}$ $^{2AB\alpha}$
petunidin 3-*O*-glucoside	$8.76 \times 10^{-4} \pm 6.0 \times 10^{-5}$ $^{1A\alpha}$	$6.10 \times 10^{-3} \pm 1.9 \times 10^{-4}$ $^{2A\alpha}$	$7.86 \times 10^{-3} \pm 5.4 \times 10^{-4}$ $^{2AB\alpha}$
peonidin 3-*O*-glucoside	$4.89 \times 10^{-4} \pm 6.8 \times 10^{-6}$ $^{1A\alpha}$	$4.40 \times 10^{-3} \pm 1.5 \times 10^{-5}$ $^{2A\alpha}$	$3.10 \times 10^{-3} \pm 4.1 \times 10^{-4}$ $^{2B\alpha}$
cyanidin 3-*O*-glucoside	$1.15 \times 10^{-3} \pm 1.3 \times 10^{-4}$ $^{1A\alpha\beta}$	$7.41 \times 10^{-3} \pm 6.7 \times 10^{-4}$ $^{2A\alpha}$	$6.76 \times 10^{-3} \pm 1.5 \times 10^{-4}$ $^{2AB\alpha}$
100 ppm AA Hot Fill			
delphinidin 3-*O*-glucoside	$5.40 \times 10^{-4} \pm 6.5 \times 10^{-5}$ $^{1A\alpha}$	$2.00 \times 10^{-3} \pm 3.2 \times 10^{-4}$ $^{2A\beta}$	$1.89 \times 10^{-3} \pm 3.7 \times 10^{-4}$ $^{2A\beta}$
malvidin 3-*O*-glucoside	$3.78 \times 10^{-4} \pm 2.4 \times 10^{-5}$ $^{1A\alpha}$	$1.34 \times 10^{-3} \pm 1.1 \times 10^{-4}$ $^{2A\beta}$	$1.01 \times 10^{-3} \pm 2.4 \times 10^{-4}$ $^{2A\beta}$
petunidin 3-*O*-glucoside	$5.05 \times 10^{-4} \pm 4.6 \times 10^{-5}$ $^{1A\alpha}$	$7.99 \times 10^{-4} \pm 6.0 \times 10^{-5}$ $^{1A\beta}$	$1.63 \times 10^{-3} \pm 3.1 \times 10^{-4}$ $^{2A\beta\delta}$
peonidin 3-*O*-glucoside	$3.03 \times 10^{-4} \pm 2.5 \times 10^{-5}$ $^{1A\alpha}$	$1.30 \times 10^{-3} \pm 1.6 \times 10^{-4}$ $^{2A\beta}$	$1.24 \times 10^{-3} \pm 3.0 \times 10^{-4}$ $^{2A\beta\delta}$
cyanidin 3-*O*-glucoside	$7.75 \times 10^{-4} \pm 4.5 \times 10^{-5}$ $^{1A\alpha}$	$2.16 \times 10^{-3} \pm 8.0 \times 10^{-5}$ $^{2A\beta\delta}$	$2.20 \times 10^{-3} \pm 1.1 \times 10^{-4}$ $^{2A\beta\varepsilon}$
500 ppm AA Hot Fill			
delphinidin 3-*O*-glucoside	$1.00 \times 10^{-3} \pm 7.5 \times 10^{-5}$ $^{1A\alpha}$	$1.51 \times 10^{-3} \pm 2.6 \times 10^{-4}$ $^{1AB\beta}$	$1.66 \times 10^{-3} \pm 1.9 \times 10^{-4}$ $^{1AB\beta}$
malvidin 3-*O*-glucoside	$5.64 \times 10^{-4} \pm 5.5 \times 10^{-5}$ $^{1A\alpha}$	$6.57 \times 10^{-4} \pm 2.2 \times 10^{-4}$ $^{1A\beta}$	$1.15 \times 10^{-3} \pm 7.6 \times 10^{-5}$ $^{2A\beta}$
petunidin 3-*O*-glucoside	$8.07 \times 10^{-4} \pm 4.9 \times 10^{-5}$ $^{1A\alpha}$	$1.13 \times 10^{-3} \pm 1.4 \times 10^{-4}$ $^{1AB\beta}$	$1.71 \times 10^{-3} \pm 1.2 \times 10^{-4}$ $^{1AB\beta\delta}$
peonidin 3-*O*-glucoside	$5.69 \times 10^{-4} \pm 2.7 \times 10^{-5}$ $^{1A\alpha}$	$7.28 \times 10^{-4} \pm 1.3 \times 10^{-4}$ $^{1AB\beta}$	$1.41 \times 10^{-3} \pm 1.1 \times 10^{-4}$ $^{2AB\beta\delta}$
cyanidin 3-*O*-glucoside	$1.29 \times 10^{-3} \pm 2.3 \times 10^{-5}$ $^{1A\alpha\beta}$	$1.74 \times 10^{-3} \pm 1.2 \times 10^{-4}$ $^{1B\beta}$	$2.46 \times 10^{-3} \pm 1.1 \times 10^{-4}$ $^{1B\beta}$
Vitamin-Enriched Water			
delphinidin 3-*O*-glucoside	$1.36 \times 10^{-3} \pm 7.2 \times 10^{-4}$ $^{1A\alpha}$	$2.26 \times 10^{-3} \pm 5.1 \times 10^{-4}$ $^{1A\beta}$	$3.45 \times 10^{-3} \pm 5.6 \times 10^{-4}$ $^{1AB\beta}$
malvidin 3-*O*-glucoside	$4.12 \times 10^{-4} \pm 2.4 \times 10^{-4}$ $^{1A\alpha}$	$6.71 \times 10^{-4} \pm 2.3 \times 10^{-4}$ $^{1A\beta}$	$1.48 \times 10^{-3} \pm 2.9 \times 10^{-4}$ $^{2A\beta}$
petunidin 3-*O*-glucoside	$1.27 \times 10^{-3} \pm 3.1 \times 10^{-4}$ $^{1A\alpha}$	$1.72 \times 10^{-3} \pm 2.5 \times 10^{-4}$ $^{1A\beta}$	$2.81 \times 10^{-3} \pm 2.5 \times 10^{-4}$ $^{2AB\beta}$
peonidin 3-*O*-glucoside	$1.05 \times 10^{-3} \pm 4.6 \times 10^{-4}$ $^{1A\alpha}$	$1.08 \times 10^{-3} \pm 1.5 \times 10^{-4}$ $^{1A\beta}$	$1.92 \times 10^{-3} \pm 3.0 \times 10^{-4}$ $^{1AB\alpha\beta}$
cyanidin 3-*O*-glucoside	$2.50 \times 10^{-3} \pm 1.8 \times 10^{-4}$ $^{1A\beta}$	$3.44 \times 10^{-3} \pm 1.1 \times 10^{-4}$ $^{1A\delta}$	$4.83 \times 10^{-3} \pm 8.7 \times 10^{-5}$ $^{2B\delta}$
Preserved Model			
delphinidin 3-*O*-glucoside	$1.21 \times 10^{-3} \pm 1.6 \times 10^{-4}$ $^{1A\alpha}$	$9.12 \times 10^{-4} \pm 7.1 \times 10^{-5}$ $^{1A\beta}$	$1.01 \times 10^{-3} \pm 1.2 \times 10^{-4}$ $^{1A\beta}$
malvidin 3-*O*-glucoside	$7.64 \times 10^{-4} \pm 1.0 \times 10^{-4}$ $^{1AB\alpha}$	$3.19 \times 10^{-4} \pm 4.5 \times 10^{-5}$ $^{1AB\beta}$	$3.33 \times 10^{-4} \pm 2.1 \times 10^{-5}$ $^{1B\beta}$
petunidin 3-*O*-glucoside	$1.16 \times 10^{-3} \pm 1.2 \times 10^{-4}$ $^{1AB\alpha}$	$7.15 \times 10^{-4} \pm 6.3 \times 10^{-5}$ $^{1AB\beta}$	$7.27 \times 10^{-4} \pm 2.0 \times 10^{-5}$ $^{1AB\delta}$
peonidin 3-*O*-glucoside	$5.80 \times 10^{-4} \pm 7.1 \times 10^{-5}$ $^{1B\alpha}$	$2.52 \times 10^{-4} \pm 1.1 \times 10^{-5}$ $^{1B\beta}$	$3.01 \times 10^{-4} \pm 3.7 \times 10^{-5}$ $^{1B\delta}$
cyanidin 3-*O*-glucoside	$9.55 \times 10^{-4} \pm 6.2 \times 10^{-5}$ $^{1AB\alpha}$	$8.83 \times 10^{-4} \pm 2.3 \times 10^{-5}$ $^{1A\beta}$	$1.03 \times 10^{-3} \pm 6.3 \times 10^{-5}$ $^{1A\varepsilon}$

[a]VEW model beverage (pH 3.60 ± 0.02) contained 0.025% ascorbic acid (AA) and 0.044% vitamin water powdered premix. All hot filled model beverages (pH 3.60 ± 0.02) contained 0.60% citric acid and 1.00% sodium citrate, with various concentrations of AA indicated in the table. Preserved model beverage (pH 3.00 ± 0.02) contained 0.05% sodium benzoate, 0.01% potassium sorbate, 2% citric acid, and 0.60% sodium citrate. Different bold superscript numbers indicate significant differences ($P < 0.05$) between light intensities within each model beverage and anthocyanin. Different bold superscript Roman letters indicate significant differences ($P < 0.05$) between anthocyanins within each light intensities and model beverage. Different bold superscript Greek letters indicate significant differences ($P < 0.05$) between model beverages within each light intensities and anthocyanin.

monomeric anthocyanin degradation rates of PSP and grape under photostress both followed first-order kinetics in the VEW model beverage (Figure 4). Correlation coefficients for PSP extract in the VEW model were 0.74, 0.90, and 0.93 for 250, 500, and 750 W/m^2 treatments, respectively. At 250 and 500 W/m^2, total monomeric anthocyanin degradation occurred significantly more rapidly with PSP than with grape (Table 4). Previous studies report that acylated anthocyanins are more stable than nonacylated anthocyanins.[20,28] For example, Hayashi et al. examined the impact of 8.8 W/m^2 (254 nm) on 19 anthocyanin-rich extracts in a pH 3.16 buffer for 18 h.[28] Furthermore, they analyzed samples on the basis of their absorbance at 525 nm, which is a measurement of the color of anthocyanins and may not necessarily be proportional to anthocyanin content, particularly with acylated anthocyanins, which undergo intramolecular copigmentation interactions. In the present study we used much greater light intensities at a range of wavelengths and different solutions and analyzed the degradation of anthocyanins not on the basis of the color but rather on the basis of the total monomeric anthocyanin concentration and individual anthocyanins by LC-MS.

Our LC-MS analysis indicated that several pigments were increasing in concentration when exposed to photostress but not thermostress. Morais et al. previously reported the formation of new pigments after anthocyanin-rich grape extracts were exposed to photostress; however, the anthocyanins and the formed pigments were not identified.[29] Three acylated peondins with elution times between 20.4 and 22.5 min were decreasing in concentration, whereas three others with elution times between 23.3 and 25.0 min were increasing in concentration (Figure 5). These peonidins were tentatively identified on the basis of parent ions and α-cleavage fragmentations from TOF experiments.[4,30] For example, peonidin-3-dicaffeoylsophoroside-5-glucoside was identified on the basis of a parent ion of 1111 and fragments ions m/z 949, 463, and 301 corresponding to the removal of caffeic acid and/or glycosides (Table 1). The degraded compounds were identified as diacylated peonidins, specifically peonidin-3-dicaffeoylsophoroside-5-glucoside, peonidin-3-caffeoyl-*p*-hydroxybenzoylsophoroside-5-glucoside, and peonidin-3-caffeoylferuloylsophoroside-5-glucoside. The three forming compounds were tentatively identified as monoacylated peonidins, specifically peonidin-3-caffeoylsophoroside-5-glucoside, peonidin-3-*p*-hydroxybenzoylsophoroside-5-glucoside, and peonidin-3-feruloylsophoroside-5-glucoside. Thus, it is likely that the photostress induced the removal of caffeic acid from the

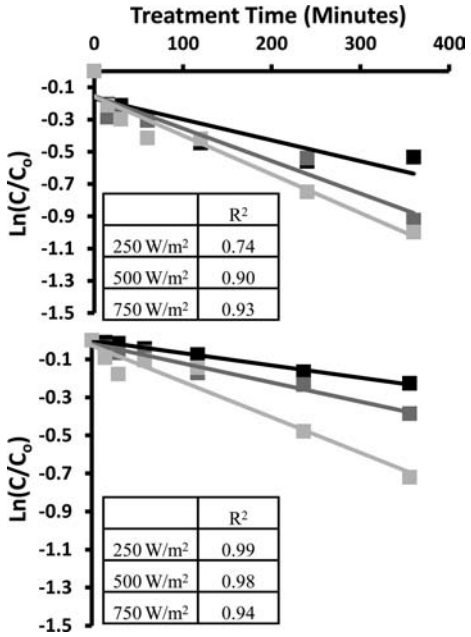

Figure 4. Total monomeric anthocyanin first-order kinetic plots for PSP (top) and grape (bottom) in VEW model beverages during phototreatment. Black, dark gray, and light gray squares correspond to 250, 500, and 750 W/m^2 treatments, respectively. "C" and "C$_0$" are the total monomeric anthocyanins concentration at a given time and the initial time, respectively.

diacylated peonidins to yield the monoacylated peonidins. However, the concentration of peonidin-3-sophoroside-5-glucoside did not increase, indicating that monoacylated peonidins do not undergo a similar degradation mechanism. Furthermore, only one isomer of peonidin-3-caffeoylsophoroside-5-glucoside (*m*/*z* 949) was detected, indicating that the photodegradative mechanism of peonidin-3-dicaffeoylsophoroside-5-glucoside involved the removal of caffeic acid from a specific position. Matsufuji et al. demonstrated that red radish extract containing seven diacylated pelargonidins will form seven new unidentified pigments when exposed to light and hypothesized that they were isomers.[31] However, they obtained only UV−vis spectra and not mass spectra; thus, they were unable to test their hypothesis. From our findings, it is possible that some or all of these new pigments were monoacylated derivatives of the original seven diacylated pelargonidins. However, unlike our findings, Matsufuji et al. also detected several of these new pigments through thermotreatments. Although this research is a step toward comprehending the chemistry of acylated anthocyanins, more research is required to fully understand the mechanisms involved.

In conclusion, the present study demonstrates the degradation kinetics of anthocyanins in the models of common RTD beverage formats through thermo- and photostress. Greater intensities of either stress resulted in increased degradation rates of both total monomeric anthocyanins and individual anthocyanidin 3-*O*-glucosides. Additionally, AA increased the degradation rates through thermostress but decreased degradation rates through photostress. Finally, photostress resulted in the removal of a caffeic acid moiety from diacylated peonidins to form monoacylated analogues. These findings are likely to contribute to the development of strategies for the formulation of anthocyanins and anthocyanin-rich ingredients in RTD beverages.

AUTHOR INFORMATION

Corresponding Author

*Phone: 1 (765) 494-0625. Fax: 1 (765) 494-7953. E-mail: mferruzz@purdue.edu.

Notes

The authors declare no competing financial interest.

REFERENCES

(1) Radomski, J. L. Toxicology of food colors. *Annu. Rev. Pharmacol.* **1974**, *14*, 127−137.

(2) Bateman, B.; Warner, J. O.; Hutchinson, E.; Dean, T.; Rowlandson, P.; Gant, C.; Grundy, J.; Fitzgerald, C.; Stevenson, J.

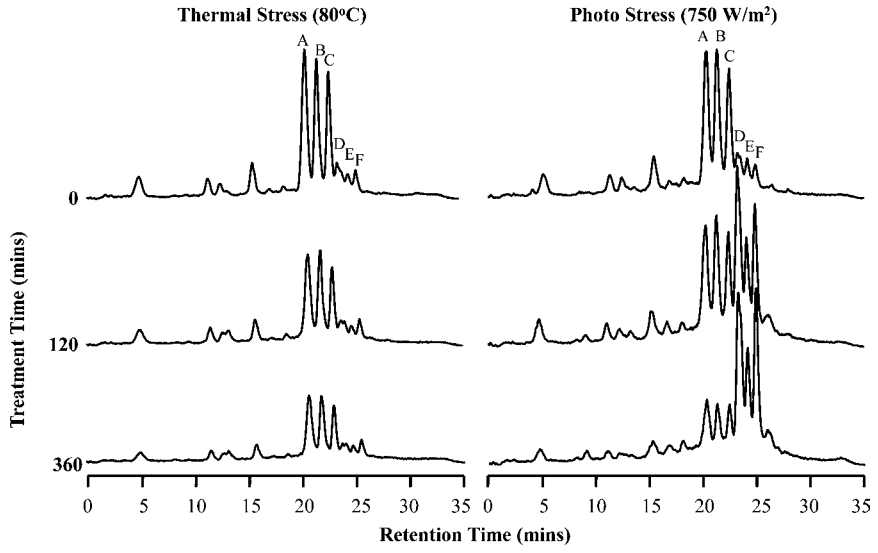

Figure 5. Normalized extracted ion chromatograms for peonidins (*m*/*z* 301) through thermostress (left) and photostress (right) at 0, 120, and 360 min. Labels A−F correspond to peonidin-3-dicaffeoylsophoroside-5-glucoside, -3-caffeoyl-*p*-hydroxybenzoylsophoroside-5-glucoside, -3-caffeoylferuloylsophoroside-5-glucoside, -3-caffeoylsophoroside-5-glucoside, -3-*p*-hydroxybenzoylsophoroside-5-glucoside, and -3-feruloylsophoroside-5-glucoside, respectively. D, E, and F increase in peak area during photo- but not thermostress.

The effects of a double blind, placebo controlled, artificial food colourings and benzoate preservative challenge on hyperactivity in a general population sample of preschool children. *Arch. Dis. Child.* **2004**, *89*, 506−511.
(3) Gavrilova, V.; Kajdzanoska, M.; Gjamovski, V.; Stefova, M. Separation, characterization and quantification of phenolic compounds in blueberries and red and black currants by HPLC-DAD-ESI-MS^n. *J. Agric. Food Chem.* **2011**, *59*, 4009−4018.
(4) Truong, V. D.; Deighton, N.; Thompson, R. T.; McFeeters, R. F.; Dean, L. O.; Pecota, K. V.; Yencho, G. C. Characterization of anthocyanins and anthocyanidins in purple-fleshed sweetpotatoes by HPLC-DAD/ESI-MS/MS. *J. Agric. Food Chem.* **2010**, *58*, 404−410.
(5) Chen, A. F.; Chen, D. D.; Daiber, A.; Faraci, F. M.; Li, H.; Rembold, C. M.; Laher, I. Free radical biology of the cardiovascular system. *Clin. Sci. (London)* **2012**, *123*, 73−91.
(6) Ghiselli, A.; Nardini, M.; Baldi, A.; Scaccini, C. Antioxidant activity of different phenolic fractions separated from an Italian red wine. *J. Agric. Food Chem.* **1998**, *46*, 361−367.
(7) Wang, H.; Cao, G.; Prior, R. L. Oxygen radical absorbing capacity of anthocyanins. *J. Agric. Food Chem.* **1997**, *45*, 304−309.
(8) Heo, H. J.; Lee, C. Y. Strawberry and its anthocyanins reduce oxidative stress-induced apoptosis in pc12 cells. *J. Agric. Food Chem.* **2005**, *53*, 1984−1989.
(9) Shih, P. H.; Wu, C. H.; Yeh, C. T.; Yen, G. C. Protective effects of anthocyanins against amyloid β-peptide-induced damage in neuro-2a cells. *J. Agric. Food Chem.* **2011**, *59*, 1683−1689.
(10) Tiwari, B. K.; O'Donnell, C. P.; Patras, A.; Brunton, N.; Cullen, P. J. Anthocyanins and color degradation in ozonated grape juice. *Food Chem. Toxicol.* **2009**, *47*, 2824−2829.
(11) Cevallos-Casals, B. v. A.; Cisneros-Zevallos, L. Stability of anthocyanin-based aqueous extracts of Andean purple corn and red-fleshed sweet potato compared to synthetic and natural colorants. *Food Chem.* **2004**, *86*, 69−77.
(12) Wang, W.-D.; Xu, S.-Y. Degradation kinetics of anthocyanins in blackberry juice and concentrate. *J. Food Eng.* **2007**, *82*, 271−275.
(13) Kechinski, C. P.; Guimaraes, P. V.; Norena, C. P.; Tessaro, I. C.; Marczak, L. D. Degradation kinetics of anthocyanin in blueberry juice during thermal treatment. *J. Food Sci.* **2010**, *75*, C173−C176.
(14) Kırca, A.; Cemeroğlu, B. Degradation kinetics of anthocyanins in blood orange juice and concentrate. *Food Chem.* **2003**, *81*, 583−587.
(15) Giusti, M.; Wrolstad, R. E. Characterization and measurement of anthocyanins by UV-visible spectroscopy. In *Current Protocols in Food Analytical Chemistry*; Wrolstad, R. E., Ed.; Wiley: New York; 2001; 1, pp F1.2.1−F1.2.13.
(16) Cemeroglu, B.; Velioglu, S.; Isik, S. Degradation kinetics of anthocyanins in sour cherry juice and concentrate. *J. Food Sci.* **1994**, *59*, 1216−1218.
(17) Manso, M. C.; Oliveira, F. A. R.; Oliveira, J. C.; Frías, J. M. Modelling ascorbic acid thermal degradation and browning in orange juice under aerobic conditions. *Int. J. Food Sci. Technol.* **2001**, *36*, 303−312.
(18) Calvi, J. P.; Francis, F. J. Stability of concord grape (v. Labrusca) aanthocyanins in model systems. *J. Food Sci.* **1978**, *43*, 1448−1456.
(19) Talcott, S. T.; Brenes, C. H.; Pires, D. M.; Del Pozo-Insfran, D. Phytochemical stability and color retention of copigmented and processed muscadine grape juice. *J. Agric. Food Chem.* **2003**, *51*, 957−963.
(20) Dyrby, M.; Westergaard, N.; Stapelfeldt, H. Light and heat sensitivity of red cabbage extract in soft drink model systems. *Food Chem.* **2001**, *72*, 431−437.
(21) Harper, K. A.; Morton, A. D.; Rolfe, E. J. The phenolic compounds of blackcurrant juice and their protective effect on ascorbic acid. *Int. J. Food Sci. Technol.* **1969**, *4*, 255−267.
(22) García-Viguera, C.; Bridle, P. Influence of structure on colour stability of anthocyanins and flavylium salts with ascorbic acid. *Food Chem.* **1999**, *64*, 21−26.
(23) Poei-Langston, M. S.; Wrolstad, R. E. Color degradation in an ascorbic acid-anthocyanin-flavanol model system. *J. Food Sci.* **1981**, *46*, 1218−1236.
(24) Attoe, E. L.; Von Elbe, J. H. Photochemial degradation of betanine and selected anthocyanins. *J. Food Sci.* **1981**, *46*, 1934−1937.
(25) Bassa, L. A.; Francis, F. J. Stability of anthocyanins from sweet potatoes in a model beverage. *J. Food Sci.* **1987**, *52*, 1753−1754.
(26) Malien-Aubert, C.; Dangles, O.; Amiot, M. J. Color stability of commercial anthocyanin-based extracts in relation to the phenolic composition. Protective effects by intra- and intermolecular copigmentation. *J. Agric. Food Chem.* **2001**, *49*, 170−176.
(27) Kırca, A.; Özkan, M.; Cemeroğlu, B. Effects of temperature, solid content and pH on the stability of black carrot anthocyanins. *Food Chem.* **2007**, *101*, 212−218.
(28) Hayashi, K.; Ohara, N.; Tsukui, A. Stability of anthocyanins in various vegetables and fruits. *Food Sci. Technol. Int.* **1996**, *2*, 30−33.
(29) Morais, H.; Ramos, C.; Forgacs, E.; Cserhati, T.; Oliviera, J. Influence of storage conditions on the stability of monomeric anthocyanins studied by reversed-phase high-performance liquid chromatography. *J. Chromatogr., B: Anal. Technol. Biomed. Life Sci.* **2002**, *770*, 297−301.
(30) Montilla, E. C.; Hillebrand, S.; Butschbach, D.; Baldermann, S.; Watanabe, N.; Winterhalter, P. Preparative isolation of anthocyanins from Japanese purple sweet potato (*Ipomoea batatas* L.) varieties by high-speed countercurrent chromatography. *J. Agric. Food Chem.* **2010**, *58*, 9899−9904.
(31) Matsufuji, H.; Kido, H.; Misawa, H.; Yaguchi, J.; Otsuki, T.; Chino, M.; Takeda, M.; Yamagata, K. Stability to light, heat, and hydrogen peroxide at different pH values and DPPH radical scavenging activity of acylated anthocyanins from red radish extract. *J. Agric. Food Chem.* **2007**, *55*, 3692−3701.